Biochimica et Biophysica Acta 1818 (2012) 425–433

Contents lists available at SciVerse ScienceDirect

Biochimica et Biophysica Acta

journal homepage: www.elsevier.com/locate/bbamem

StarD7 behaves as a fusogenic protein in model and cell membrane bilayers ☆

Sofía Angeletti [a,b,1], Julieta M. Sanchez [a,1], Larry W. Chamley [c], Susana Genti-Raimondi [b], María A. Perillo [a,*]

[a] Biofísica-Química, Cátedra de Química Biológica, Dpto. Química. Facultad de Ciencias Exactas, Físicas y Naturales, Argentina
[b] Dpto. Bioquímica Clínica-CIBICI, Facultad de Ciencias Químicas. Universidad Nacional de Córdoba, Argentina
[c] Department of Obstetrics and Gynaecology, School of Medicine, Faculty of Medical and Health Sciences, The University of Auckland, New Zealand

ARTICLE INFO

Article history:
Received 10 August 2011
Received in revised form 18 October 2011
Accepted 19 October 2011
Available online 28 October 2011

Keywords:
StarD7
Bilayer fusion
Steady state fluorescence de-quenching
Dynamic light scattering
FRET
Trophoblast syncytialisation

ABSTRACT

StarD7 is a surface active protein, structurally related with the START lipid transport family. So, the present work was aimed at elucidating a potential mechanism of action for StarD7 that could be related to its interaction with a lipid–membrane interface. We applied an assay based on the fluorescence de-quenching of BD-HPC-labeled DMPC–DMPS 4:1 mol/mol SUVs (donor liposomes) induced by the dilution with non-labeled DMPC–DMPS 4:1 mol/mol LUVs (acceptor liposomes). Recombinant StarD7 accelerated the dilution of BD-HPC in a concentration-dependent manner. This result could have been explained by either a bilayer fusion or monomeric transport of the labeled lipid between donor and acceptor liposomes. Further experiments (fluorescence energy transfer between DPH-HPC/BD-HPC, liposome size distribution analysis by dynamic light scattering, and the multinuclear giant cell formation induced by recombinant StarD7) strongly indicated that bilayer fusion was the mechanism responsible for the StarD7-induced lipid dilution. The efficiency of lipid dilution was dependent on StarD7 electrostatic interactions with the lipid–water interface, as shown by the pH- and salt-induced modulation. Moreover, this process was favored by phosphatidylethanolamine which is known to stabilize non-lamellar phases considered as intermediary in the fusion process. Altogether these findings allow postulate StarD7 as a fusogenic protein.

1. Introduction

Membrane fusion is a ubiquitous event in cell biology, and indeed potentially all membranes can be merged under appropriate conditions. Fusion is involved in processes such as fertilization, cell differentiation (myoblasts and trophoblasts), transport of vesicles and protein-mediated virus entry to host cells. Many effectors are involved in the fusion process (e.g. intrinsic and extrinsic membrane proteins [1]; calcium, in exocytosis [2]; hormones, growth factors and antibodies, in receptor-mediated endocytosis [3]; pH, during the invasion of viruses [4]; etc.). While it is known that proteins and other factors are essential in controlling the membrane fusion process, lipids are the ultimate actors in this phenomenon. There are some lipids such as lysophosphatidylcholine, monoglycerides, phosphatidylethanolamine and phosphatidylserine that have been postulated as fusogenic in model membranes because they play a key role in membrane fusion [5]. However, it is unlikely that a particular lipid can be fully responsible for fusion in natural cell membranes.

The transport of lipids and proteins between organelles is also an essential process in the organization of different cellular compartments. Phospholipids are predominantly synthesized in the endoplasmic reticulum and subsequently transported to various destinations by vesicular transport through the fusion of vesicles to an acceptor compartment or can also be delivered to specific cellular organelles by monomeric exchange [6]. Several cytosolic proteins with specific lipid binding domains capable of accelerating lipid exchange in vitro have been identified. Based upon the homology in the domain responsible for interacting with the lipids, these proteins are grouped into six families called CRAL/TRIO, PITP, ORP, GLTP, SCP and START [7]. Crystallographic studies on the START domain of different members of this superfamily show that the three-dimensional organization of the domain forms a hydrophobic tunnel which is wide enough to accommodate the lipid molecule [6,8,9].

StarD7 is a member of the START domain protein family. Recombinant StarD7 protein is a surface active protein capable of interacting with lipid monolayers, particularly with negatively charged phospholipids such as phosphatidylserine and phosphatidylglycerol [10].

Abbreviations: DPH-HPC, 2-(3-(diphenylhexatrienyl) propanoyl)-1-hexadecanoyl-sn-glycero-3-phosphocholine; BODIPY-FL-C5-HPC (also BD-HPC), 2-(4,4-difluoro-5,7-dimethyl-4-bora-3a,4a-diaza-s-indacene-3-pentanoyl)-1-hexadecanoyl-sn-glycero-3-phosphocholine; DLS, dynamic light scattering; DMPC, dimiristoylphosphatidylcholine; DMPS, dimiristoylphosphatidylserine; DMPE, dimiristoylphosphatidylethanolamine; StarD7, StAR-related lipid transfer (START) domain containing 7; LUVs, large unilamellar vesicles; FRET, fluorescence energy transfer; MLVs, multilamellar vesicles; PC, phosphatidylcholine; PS, phosphatidylserine; PE, phosphatidylethanolamine; START, StAR-related lipid transfer; StAR, steroidogenic acute regulatory protein; SUVs, small unilamellar vesicles.

☆ The present work was partially financed by grants from CONICET, SECyT-Universidad Nacional de Córdoba and ANPCyT from Argentina.

* Corresponding author. Tel.: +54 351 4344983x5; fax: +54 351 4334139.
E-mail address: mperillo@efn.uncor.edu (M.A. Perillo).

[1] These authors contributed equally to the present work.

0005-2736/$ – see front matter © 2011 Elsevier B.V. All rights reserved.
doi:10.1016/j.bbamem.2011.10.024

A recent study demonstrated that the overexpression of StarD7 in a mouse hepatoma cell line induced the increase in the intracellular transport of exogenously incorporated phosphatidylcholine (PC) into the mitochondria. Although it was suggested that StarD7 facilitated the delivery of PC to mitochondria in non-vesicular form, the precise mechanism by which PC was trafficked remained to be elucidated [11]. Moreover, there is an increase in StarD7 expression and partial relocalization from the cytoplasm to the plasma membrane during syncytialisation, in vitro, of primary cytotrophoblasts from human placentae [12]. Syncytialisation is a differentiation process, which involves the intercellular fusion of trophoblast cells, concomitant with the translocation of phosphatidylserine from the inner to the outer leaflet of the trophoblast plasma membranes [13]. To interpret these results there might be two scenarios: a) StarD7 is involved in trophoblast differentiation through the transport of phosphatidylserine through the START domain [12] and/or b) StarD7 induces structural changes in the bilayer phase leading to membrane fusion. Based on its structural homology with other proteins of the START family, StarD7 might be postulated as a lipid carrier protein. However, an effect of StarD7 on trophoblast syncytialisation would support the protein has a fusogenic activity.

The present work was aimed at elucidating the mechanism of action of StarD7 derived from its interaction with a lipid–membrane interface.

2. Materials and methods

2.1. Materials

StarD7 (MW 34,697 Da), with a 95% purity as evidenced by SDS-PAGE, was overexpressed in *Escherichia coli* and purified as described previously [10]. The acyl chain labeled fluorescent probes (Fig. 1) DPH-HPC and BODIPY-FL-C5-HPC (BD-HPC) were purchased from Molecular Probes, Inc (Eugene, OR) and Avanti Polar lipids (Alabaster, AL), respectively. DMPC, DMPE and DMPS were purchased from Avanti Polar lipids (Alabaster, AL). Other chemicals were of analytical grade. Ultrapurified water was used all through the experiments.

2.2. Fluorescence measurements

Fluorescence spectra were recorded with a Fluoromax Spex-3 Jovin Yvon (Horiba, NJ, USA) spectrofluorimeter equipped with a thermostatized cell, a Xe arc lamp and a photomultiplier tube as signal detector, where light intensity was registered by a photon counting system. The excitation and emission slits were 2 nm wide. Emission spectra were recorded between 500 nm and 600 nm at 490 nm excitation wavelength.

2.3. Multilamellar vesicle (MLV) preparation

Lipids were dissolved in chloroform/methanol (2:1 v/v). The solvent was then evaporated under a stream on nitrogen with constant rotation of a test tube so as to deposit a uniform film over the bottom third of a tube and traces of solvent were removed under vacuum. The film was hydrated with 20 mM Tris–HCl, pH 7.8 by vortexing at a temperature above the gel to liquid-crystalline phase transition temperature of the lipids to obtain MLVs. The composition of "Donor" and "Acceptor" vesicles and their relative proportions used in the present work was as reported [14,15].

2.4. Donor liposomes

Small unilamellar vesicles (SUVs) were prepared essentially according to Pereira-Lachataignerais and co-workers [16] using a high intensity sonicator series Autotune, model 130 W with a 3 mm-diameter titanium probe and at a high frequency of 20 kHz. Ten mL of MLV dispersion containing 1:3.6 (mol/mol) mixture of BD-HPC (40 nM, final concentration) with phospholipids (DMPC–DMPS 4:1 mol/mol) was sonicated for 50 min (50 pulses with intervals of 15 s.) at 30 W in a 15 mL tube maintained on ice. Thus, labeled SUVs ($SUV_{BD\text{-}HPC/PC/PS}$) were obtained and used as donor liposomes. Non-labeled SUVs ($SUV_{PC/PS}$) were also prepared by applying the same procedure but in the absence of BD-HPC. Samples were centrifuged at 10,000 rpm for 2 min in order to release titanium particles and maintained covered with aluminum foil to prevent light incidence.

2.5. Acceptor liposomes

A MLVs' suspension containing 6 μM phospholipid concentration (DMPC:DMPS 4:1) was extruded across polycarbonate 100 nm pore size filters, according to MacDonald et al. [17] with a mini-extrusor

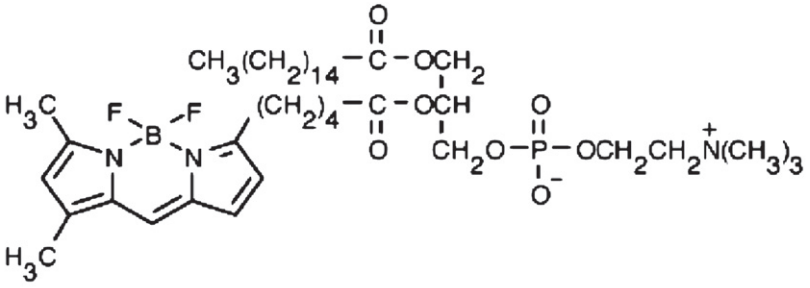

BODIPY-FL-C5-HPC

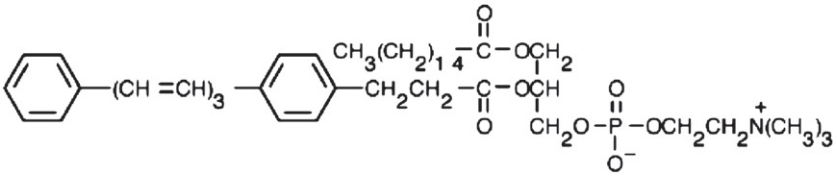

DPH-HPC

Fig. 1. Chemical structures of the fluorescence probes used.

Liposofast™-Basic Avestin (Ottawa, Canada). The large unilamellar vesicles (LUVs) obtained ($LUV_{PC/PS}$) were used as acceptor liposomes.

2.6. Effect of environmental polarity on the spectroscopic behavior of BD-HPC

BD-HPC was dispersed at 8 nM final concentration in solvents that differed in their polarity expressed by the value of their dielectric constants (D) such as water ($D_{water} = 78.36$) and aqueous dioxane solutions at 20, 45, 70 and 82% v/v dioxane concentrations ($D_{20\%\ dioxane} = 60.79$; $D_{45\%\ dioxane} = 38.48$; $D_{70\%\ dioxane} = 17.69$; $D_{82\%\ dioxane} = 9.53$) [18]. Fluorescence emission spectra were recorded between 500 and 600 nm.

BD-HPC has the dye (BODIPY FL) attached to the sn-2-acyl chain via a C5 alkyl chain. BODIPY FL can form excimers at high concentrations and unlike fluorophores like pyrene, DPH and NBD, BODIPY FL has been considered relatively environment insensitive and it is fluorescent in both aqueous and lipid environments [19,20]. However, our experiments showed its sensitivity to medium polarity (see Fig. 3 below).

2.7. Fluorescence time course in the presence of StarD7 and LUVs

A suspension of "Donor" liposomes ($SUV_{BD\text{-}HPC/PC/PS}$) was equilibrated at room temperature (23 °C) in 20 mM Tris–HCl pH 7.8 buffer (assay buffer). The effect of medium pH and ionic strength was evaluated using liposomes dispersed in 20 mM sodium acetate or 20 mM sodium phosphate, pH 6 buffers, to check the anion effect, as well as in 20 mM Tris–HCl, pH 7.8 buffer containing 500 mM NaCl. The residual fluorescence intensity (FI) of the self-quenched probe fluorescence was recorded for 10 min. Then, recombinant StarD7 protein was added at the desired concentration and recording continued for another 10 min until FI was stabilized. Finally, an excess of "Acceptor" liposome suspension ($LUV_{PC/PS}$) was added at a final concentration of 6 μM.

2.8. Fluorescence resonance energy transfer assay —FRET

Two separated LUV samples containing either DPH-HPC or BD-HPC ($LUV_{DPH\text{-}PC/PC/PS}$ and $LUV_{BD\text{-}HPC/PC/PS}$, respectively) were prepared as described above. Both samples were mixed together and the time-course of the fluorophore behavior was recorded at the BD-HPC emission maximum ($\lambda_{em} = 515$ nm) after excitation at 356 nm (the λ_{ex} of DPH-HPC), in the absence and in the presence of StarD7.

2.9. Dynamic light scattering

Liposome size distribution was determined as described previously by using a Nicomp™ 380 particle sizer (Nicomp Particle Sizer Systems, Santa Bárbara, CA) operating at 532 nm and at an average count rate between 250 and 500 kHz; run time was around 15 min for most samples. Aliquots of vesicle suspension (1 mg of lipid per mL) with or without StarD7 (35 μM) were taken for determinations. Measurements were made at 22 °C. The time autocorrelation function of scattered light intensities was analyzed by an inverse Laplace transform –ILS– algorithm to obtain a volume weighted distribution of diameters [21].

2.10. Immunofluorescence of BeWo cells

Morphological differentiation of BeWo cells (a trophoblast cell line) treated with recombinant StarD7 protein was followed by immunofluorescence microscopy to identify cell boundaries. Briefly, 8000 cells/well were cultured in Ham's F12K on 96-well plates, grown for 12 h and then incubated between 0 and 0.5 μM recombinant StarD7 in phosphate buffered saline (PBS) for 20 h. After rinsing with PBS, cells were fixed 10 min in methanol at room temperature. The cells were then rinsed with 0.2% Tween in PBS (PBST) three times and then blocked in 10% normal goat serum (NGS) PBST. After 10 min, the cells were incubated at room temperature with the mouse anti-desmosomal protein diluted in 10% NGS (ZK-31, 0.045 mg/mL, Sigma-Aldrich Inc. St. Louis, MO, USA). After 1 h, the antibody solution was removed, the cells were rinsed with PBST three times and then incubated 1 h with the Alexa Fluor 488-conjugated goat anti-mouse IgG (Molecular Probes, Inc., Eugene, OR) was applied. Cells were washed with PBST three times and nuclei were counterstained with Hoechst 33258 dye. Finally, each well was rinsed and covered with PBS to analyse by microscopy (Eclipse Ti confocal microscope, Nikon).

Intercellular fusion was quantified by counting the number of nuclei in syncytia and the total number of nuclei in an average of ten microscopic fields from each condition. The percentage of the nuclei in syncytia was determined as: (number of nuclei in syncytia/total number of nuclei) × 100, as described [22]. Duplicate wells were evaluated in each experiment, and each experiment was performed at least twice independently.

2.11. Statistical analysis

Statistical analysis was performed using the GraphPad Prism 5.0 software. One-way analysis of variance (ANOVA) followed by Dunnett's Multiple Comparison post-Test was applied and $p < 0.05$ was considered statistically significant.

3. Results

StarD7 induced a concentration-dependent increase in the FI emitted by the BD-HPC incorporated in SUV donor vesicles ($SUV_{BD\text{-}HPC/PC/PS}$) (Fig. 2). Upon StarD7 addition (first stage) at concentration ≥2 nM FI increased hyperbolically as a function of time up to a plateau (FI_{max1}). At concentrations ≤0.4 nM StarD7 did not cause any detectable effect. The subsequent addition of a fixed amount of non-labeled $LUV_{PC/PS}$ (second stage) induced a further increase in FI also following a hyperbolic time-course and finally reaching a second maximal intensity level (FI_{max2}) (Fig. 2a).

In Fig. 2b the values of FI_{max1} and FI_{max2}, determined at both plateaux, which appeared after the addition of StarD7 and $LUV_{PC/PS}$, respectively, were plotted as a function of the StarD7 concentration.

In the presence of StarD7 alone, FI_{max1} increased in a linear fashion relative to the protein concentration. The maximum dequenching achieved within the concentration range of StarD7 tested was 84.7% however, in another experiment using 10 nM StarD7 (see Control sample in Fig. 7b) a similar percentage of dequenching was reached. From these results it could be concluded that the dequenching effect cannot be completed with the sole effect of StarD7. Thus, the effect of StarD7 possibly was due to a hydrophobic environment provided by the protein to the fluorescent probe. Moreover, 100% dequenching cannot be reached due to the fact that some labeled molecules, located in the inner membrane leaflet, are not accessible to the protein. This possibility was tested by a spectroscopic analysis of the probe in media of different polarities (see below).

In contrast to the linear behavior of FI_{max1}, FI_{max2} measured in the presence of $LUV_{PC/PS}$ followed a biphasic trend with a discontinuity at ≅0.4 nM StarD7. Below this concentration the slope was steeper than in the absence of acceptor LUVs and at higher StarD7 concentrations the slope was less steep, suggesting a tendency towards saturation.

The spectra of BD-HPC emission fluorescence, depicted in Fig. 3a, exhibited a red-shift and a significant decrease in fluorescence intensity (quenching) as the medium became more polar (higher D). This behavior was observed within the whole range of D values examined and the stronger effect appeared as D increased from 60 to 80 (80 to 100% water) (Fig. 3b).

Evaluation of possible effects of lipid–protein binding on the dequenching efficiency of StarD7 is shown in Fig. 4. The dequenching effect observed at pH 7.8 after the addition of LUVs was stronger in Tris–HCl buffer (Fig. 4a) compared to phosphate buffer (Fig. 4b). It

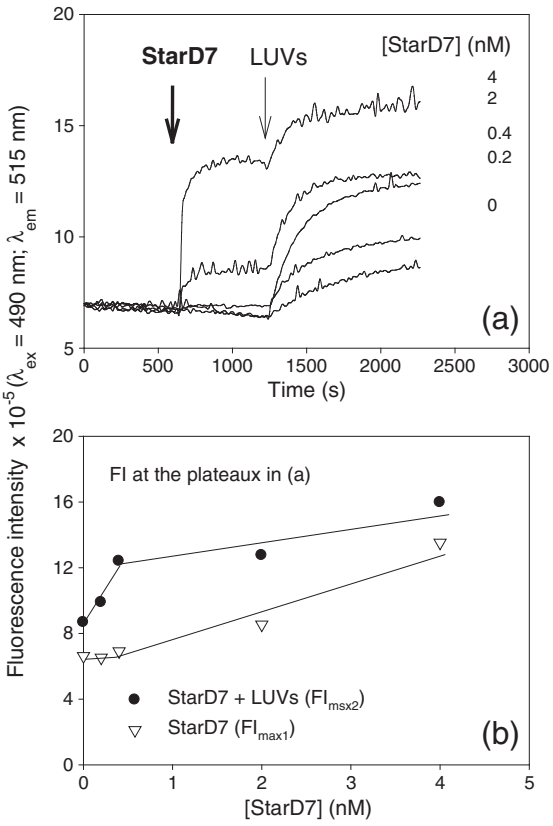

Fig. 2. StarD7 favors BD-HPC fluorescence dequenching. Fluorescence intensity of BD-HPC in DMPC–DMPS mixed SUV ($SUV_{BD\text{-}HPC/PC/PS}$) was measured as a function of StarD7 concentration. (a) Additions of StarD7 (thick arrow) and LUVs (thin arrow) are indicated. Numbers in the figure refer to StarD7 concentrations. (λ_{ex} = 490 nm and λ_{em} = 515 nm).(b) Fluorescence intensity at the plateaus: at 1000 s (▽) (after the addition of StarD7) and at 2250 s (●) (after the addition of StarD7 plus LUVs). In the text they were referred to as FI_{max1} and FI_{max2}, respectively.

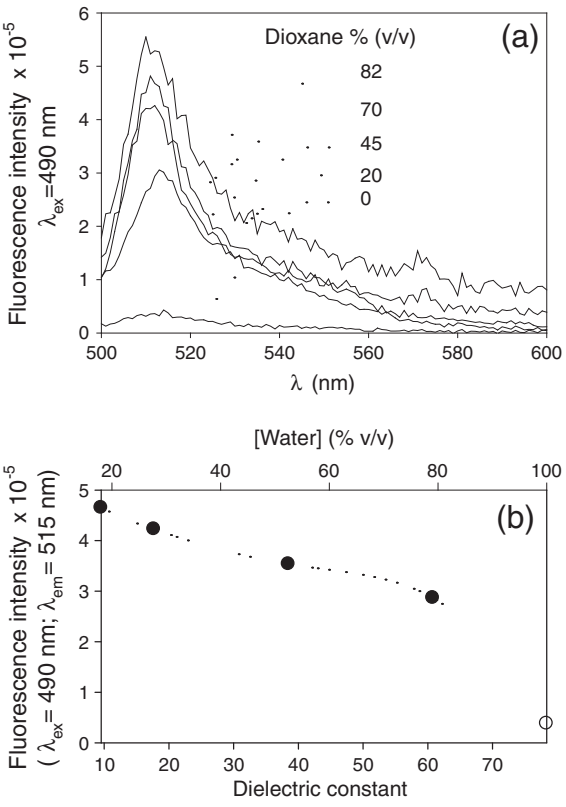

Fig. 3. Effect of medium polarity of the fluorescence emission of BD-HPC. (a) Fluorescence emission spectra were recorded at an excitation wavelength λ_{ex} = 490 nm. BD-HPC was dissolved in aqueous media containing dioxane at the concentration indicated by the numbers expressed in % v/v units. (b) Fluorescence intensity at λ_{em} = 515 nm (●) taken from spectra in panel (a) as a function of the dielectric constant (D) of the solvent (bottom x axis) or % v/v water (upper x axis).

is important to note that, at the concentrations used, the osmolarities of Tris–HCl and phosphate buffers were approximately 40 mosM and 80 mosM, respectively. The rise in the ionic strength caused by adding 500 mM NaCl leads to a total inhibition of the effect of LUVs on FI ($F_{max2} \cong 0$) (Fig. 4c). In Tris–HCl buffer pH 7.8 with StarD7 protein at 10 nM, the dequenching in the second stage (FI_{max2}) was slightly lower than in the absence of StarD7 (Fig. 4c, compare full and dotted lines). In contrast, no difference was observed when using phosphate buffer. At pH 6, close to the isoelectric point of StarD7, independent of the buffer used, acetate (Fig. 4d) or phosphate (Fig. 4e), the addition of StarD7 enhanced both F_{max1} and F_{max2}, but the final FI_{max2} levels reached were lower than at pH 7.8 (lower lipid–protein electrostatic interaction) and, as expected, F_{max2} was higher in the presence of StarD7 than in its absence.

A FRET experiment was used to evaluate whether lipid molecules merged as an intermediary stage of the bilayers undergoing fusion. As depicted in Fig. 5a, the emission spectrum of DPH-HPC ($\lambda_{ex,\ DPH\ HPC}$ = 356 nm; $\lambda_{em,\ DPH\ HPC}$ = 427 nm) overlapped the excitation spectrum of BD-HPC ($\lambda_{ex,\ BD\text{-}HPC}$ = 490 nm). This indicated that both probes would behave as a good donor/acceptor FRET couple. The high quantum yield of fluorescence, high efficiency of FRET (*Ro* is estimated to be 60 Å), photostability, and localization in the central hydrophobic region of a bilayer all make this pair of probes quite appropriate for detecting fusion. In this experiment, at the starting point, there was a mixture of two populations of LUVs labeled either with DPH-HPC or BD-HPC, and the excitation wavelength was that of DPH-HPC ($\lambda_{ex,DPH\text{-}HPC}$ = 356 nm). Fig. 5b shows the emission spectra of the LUVs mixture at different time-points (T_1 = 3 min and T_2 = 6 min). There was a decrease in 427 nm ($\lambda_{em\ DPH\text{-}HPC}$) and an increase in 515 nm ($\lambda_{em,BD\text{-}HPC}$) vs time due to probe mixing which favored Förster's energy transference from DPH-HPC (λ_{ex} = 356 nm) to BD-HPC (λ_{em} = 515). A time-course of the fluorescence intensity ratio between FI at the λ_{em} of DPH-HPC (427 nm) and FI of BD-HPC (515 nm) ($FI_{427/515}$) was then calculated (Fig. 5c). For this, a decrease in $FI_{427/515}$ was taken as an indication of FRET. Only samples containing StarD7 exhibited the decrease in $FI_{427/515}$ demonstrating that both probes, originally located in different bilayers, were able to come within the Förster's distance.

Upon bilayer fusion we anticipated finding larger particles. The measurement of the liposome size, used in the lipid dilution assay, obtained by DLS confirmed the mean particle size expected for SUVs (33 nm) and LUVs (107 nm) (Table 1). We also intended to measure the size of StarD7 molecules. However, this required the use of solutions at very high protein concentrations (35 μM) which lead to protein self-aggregation as shown by the size (547 nm) of the particles detected. It is expected that protein aggregation would not have occurred in the membrane fusion experiments (performed at 10 nM StarD7) because soluble protein monomers would be undetectable (4.39 nm diameter estimated from values of average density of proteins (δ=1.3 g/cm^3) and the molecular weight of StarD7 (MW = 34,697)) [23]. The addition of StarD7 to SUV samples induced the appearance of particles of 41 nm diameter which may result from SUV fusion (Population I, Table 1). Two peaks were observed after the addition of LUVs to SUV samples, one of them more abundant (87%) of 48 nm diameter, possibly resulting from SUV–SUV fusion (Population I), and another population (II, 13% abundance) which might represent a complex combination of several particles, including SUVs which are more unstable compared to LUVs (see Discussion).

To evaluate the occurrence of interior mixing as the latter stage of a complete fusion process, BeWo cells were cultivated with recombinant

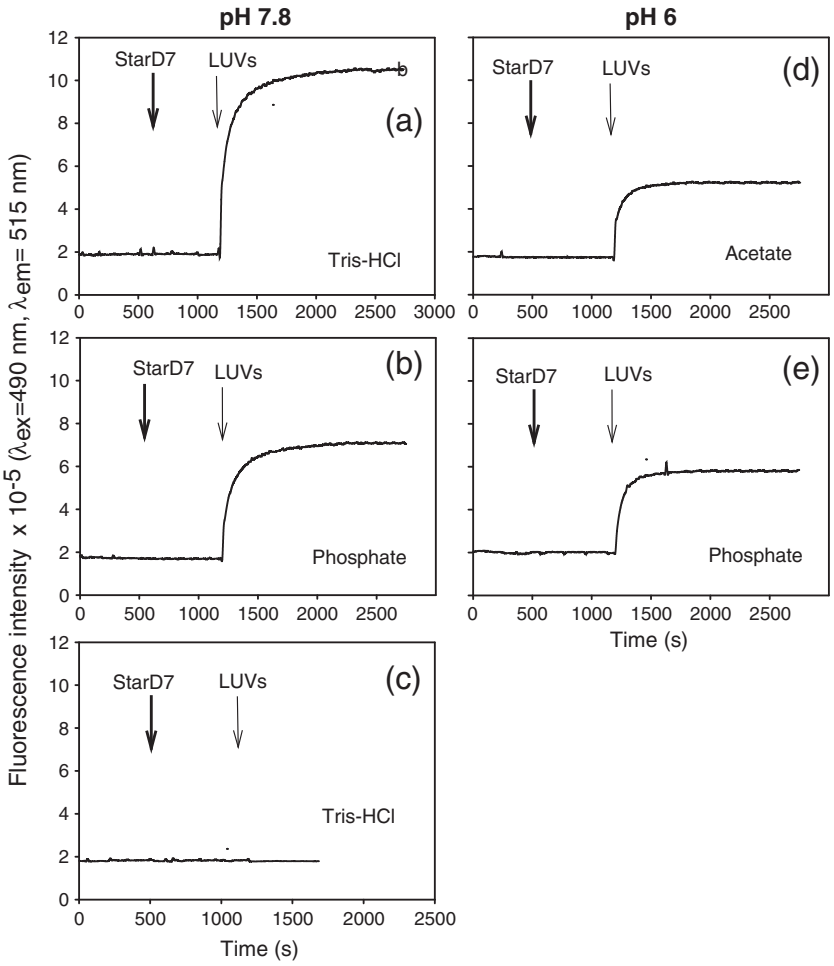

Fig. 4. Role of electrostatic interactions on the StarD7-induced BD-HPC fluorescence dequenching. The effect of pH and ionic strength of the medium on the temporal change of BD-HPC fluorescence intensity is depicted. Experiments were performed in the presence (dotted line) or in the absence (solid line) of 10 nM StarD7. Addition of StarD7 (thick arrow) and LUVs (thin arrow) is indicated. Fluorescence was recorded at $\lambda_{ex} = 490$ nm and $\lambda_{em} = 515$ nm. Solvents used for protein solution and vesicle dispersion preparations were: (a) 20 mM Tris–HCl pH 7.8 buffer; (b) 20 mM phosphate pH 7.8 buffer; (c) NaCl 500 mM in 20 mM Tris–HCl pH 7.8 buffer; (d) 20 mM acetate pH 6 buffer and (e) 20 mM phosphate pH6 buffer.

StarD7 protein for 20 h and membrane fusion was analyzed through reduction in desmoplakin protein by fluorescence microscopy. As shown in Fig. 6b, the presence of 0.5 μM StarD7 protein induced the formation of multinucleated giant cells. All the concentrations assayed exhibited an increase statistically significant with respect to the control (Fig. 6c).

The effect of a fusogenic lipid on the StarD7-induced dequenching efficiency was also tested. Similar experiments were performed to those shown above (Fig. 2). At first step, the FI changes were registered after adding either SUV_{PE-PS}, SUV_{PC-PS} or buffer (control) alone (Fig. 7a) or simultaneously with StarD7 (Fig. 7b). In the absence of StarD7 (Fig. 7a), the addition of either SUV_{PE-PS} or SUV_{PC-PS} to $SUV_{BD-HPC/PC-PS}$ induced a hyperbolic dequenching of BD-HPC fluorescence being SUV_{PE-PS} the most effective. The subsequent addition of non-labeled LUV_{PC-PS} exerted a further increase in all samples up to a similar maximum level after prolonged incubation, supporting a saturating effect. The data in Fig. 7b demonstrate that StarD7 potentiated the dequenching effect of SUV_{PC-PS} if it is compared to control experiments in the absence of StarD7 (Fig. 7a). The subsequent addition of LUV_{PC-PS}leads all samples to the same maximum of fluorescence. However, when SUV_{PE-PS} were added in the first stage, the subsequent addition of LUV_{PC-PS} in the second stage exhibited only a slight additional increase in FI reaching the same maximum with no additional increase. In the presence of PE the dequenching effect was already at a maximum level in the absence of StarD7. Thus, these results suggested that both the fusogenic PE and StarD7 exerted their dequenching effects through the same mechanism (i.e. membrane fusion). Net changes determined after each stage are synthesized in Fig. 7c. There, it is shown that the presence of PE is highly effective in inducing liposome fusion per-se. It is also noticeable that the stronger the effect in the first stage, the lower is the increment in the second stage. These findings reinforce the concept of a saturating effect in the system, underscoring the potentiating effect of StarD7 on membrane fusion, mainly observed in the other two samples (StarD7 alone and StarD7 plus SUV_{PC-PS}).

4. Discussion

In the present report we propose a function and a mechanism of action for StarD7, a protein structurally related with a protein family involved in lipid transfer processes. In doing so, we applied an experimental procedure widely considered useful to demonstrate lipid transfer from SUVs to LUVs [15]. However, considering the results from a biophysical perspective leads us to suspect the possibility that this phenomenon involves lipid dilution through a bilayer fusion. Thus, once the StarD7-induced fluorescence dequenching was demonstrated (Fig. 2) the experiments that followed aimed to show that membrane fusion is a possible mechanism explaining this result.

4.1. StarD7 stimulates BD-HPC fluorescence dequenching

StarD7 exhibited a concentration-dependent ability to increase the fluorescence intensity quantum yield of the BD-HPC present in donor

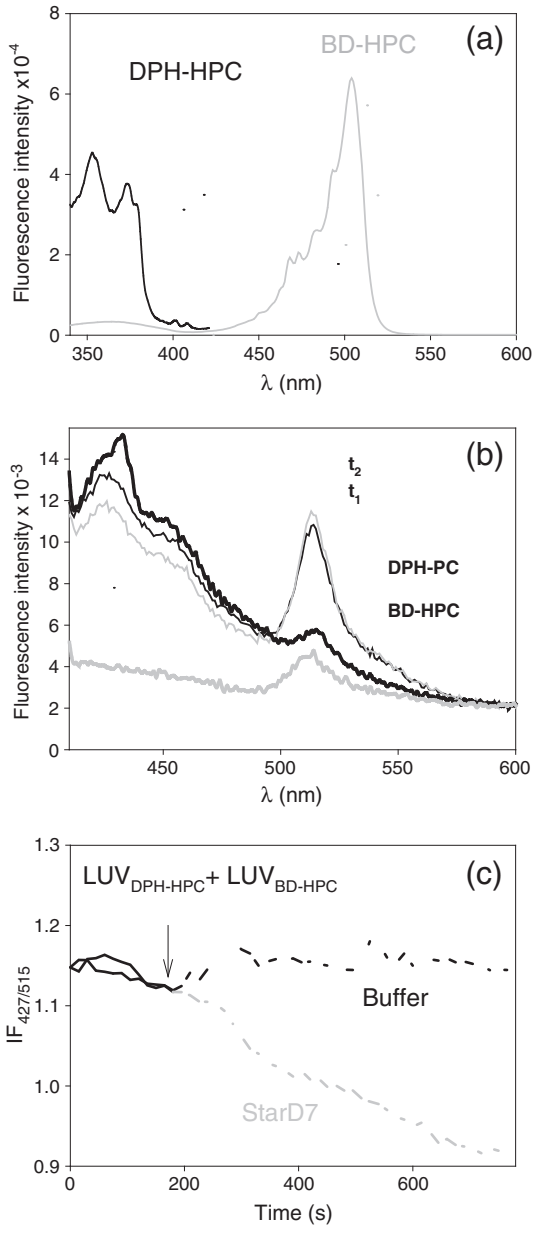

Fig. 5. StarD7 induces lipid mixing. (a) Excitation (solid lines) and emission (dotted lines) fluorescence spectra of DPH-HPC (black) and BD-HPC (gray). (b) Emission spectra of DPH-HPC (thick black line) and BD-HPC (thick gray line) alone in separate LUVs and at different times ($T_1 = 3$ min and $T_2 = 6$ min) after LUVs mixing (thin lines). (c) $FI_{427/515}$ corresponds to the fluorescence intensity ratio between FI at the λ_{em} of DPH-HPC (427 nm) and BD-HPC (515 nm). A decrease in $FI_{427/515}$ is an indication of FRET. At t_0, samples contained a mix of two different LUVs, one labeled with BD-HPC and the other one with DPH-HPC. Arrow points to further addition of 10 nM StarD7 (gray lane) or buffer (black lane).

liposomes (SUVs) (F_{max1}) and to accelerate, the dilution of labeled lipids after the addition of acceptor liposomes (LUVs) (F_{max2}) (Fig. 2). StarD7 potentiated lipid dilution following addition of LUVs even at concentrations too low to cause an effect in the presence of SUVs alone ([StarD7] ≤0.4 nM) (Fig. 2a and b). These results lead us to propose the following hypothesis: a) the linear behavior of FI_{max1}, which is an effect of StarD7 alone, is due to the probe binding within hydrophobic environments (protein pockets, protein aggregates or lipid–protein interfaces), b): the discontinuous trend of FI_{max2} does not reveal the mechanism involved in the process but reflects a tendency toward the saturation of the probe dilution effect suggesting the requirement of StarD7 binding to the lipid–water interface and c) the latter result could be a consequence of bilayer fusion, hemifusion, collapse of vesicle morphology,

Table 1
Frequency distribution analysis of mean particle diameters assessed by dynamic light scattering.

Sample	Addition	Mean particle diameter (nm)	
		Population I	Population II
$SUV_{PC/PS}$	Buffer	33 ± 3 (100)	–
$LUV_{PC/PS}$	Buffer	107 ± 1 (100)	–
StarD7[a] (35 μM)	Buffer	129 ± 20 (91)	547 ± 127 (9)
$SUV_{PC/PS}$	StarD7[b]	47 ± 4 (94.4)	326 ± 6 (5.6)
	$LUV_{PC/PS}$	48 ± 4 (87)	202 ± 5 (13)
	StarD7[b] + $LUV_{PC/PS}$	44 ± 0.1 (93)	175 ± 1.5 (7)

Numbers between brackets refer to weighted number frequency distribution.
[a] The high StarD7 concentration used in these experiments suggests that populations observed may represent different types of protein aggregates.
[b] It is expected that protein aggregation would not have occurred in these experiments because StarD7 concentration was significantly lower (10 nM).

or monomeric lipid transfer. Thus this experiment alone cannot define the mechanism by which lipid dilution occurs.

4.2. Effect of the medium polarity on BD-HPC fluorescence emission intensity

The quenching of the fluorescence intensity can be explained through a reduction in the quantum yield of the fluorophore due to the fact that non-radiative relaxation routes became faster (more favorable) compared to fluorescence. This phenomenon can be induced by the stabilization of a charge transfer state as a result of strong local electric fields near the fluorophore due to probe–probe interactions or imposed by water molecules interacting through H-bonds. It has been demonstrated that microscopic H-bonding and not the bulk dielectric constant dictates the electron transfer rate [24]. This can

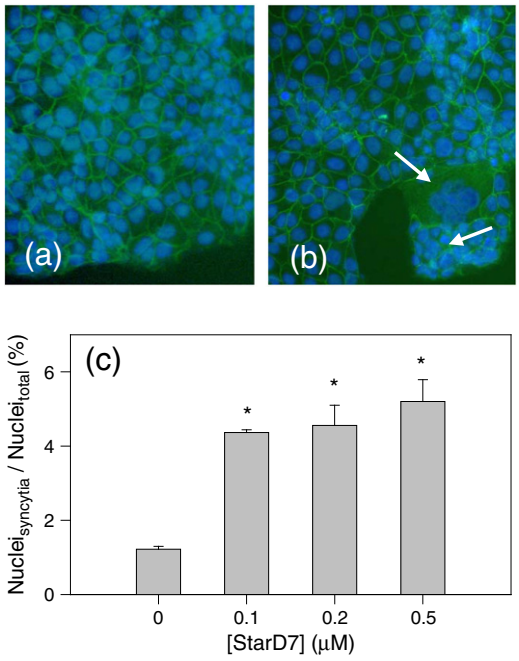

Fig. 6. StarD7 stimulates cell–cell fusion. Morphological differentiation of BeWo cells cultivated in the presence (b) or not (a) of recombinant 0.5 μM StarD7 protein. Cells were fixed and immunostained with anti-desmoplakin (green) to identify boundaries. Nuclei were stained with Hoechst dye. Arrows show syncytium-like structures. (a) As a negative control the cells were incubated with the vehicle (PBS). (c) Percentage of nuclei in syncytia with respect to total number of nuclei at different StarD7 concentrations. Results represent the mean ± SEM of three independent experiments performed in duplicate. *Significant difference ($p<0.05$) compared to the control condition.

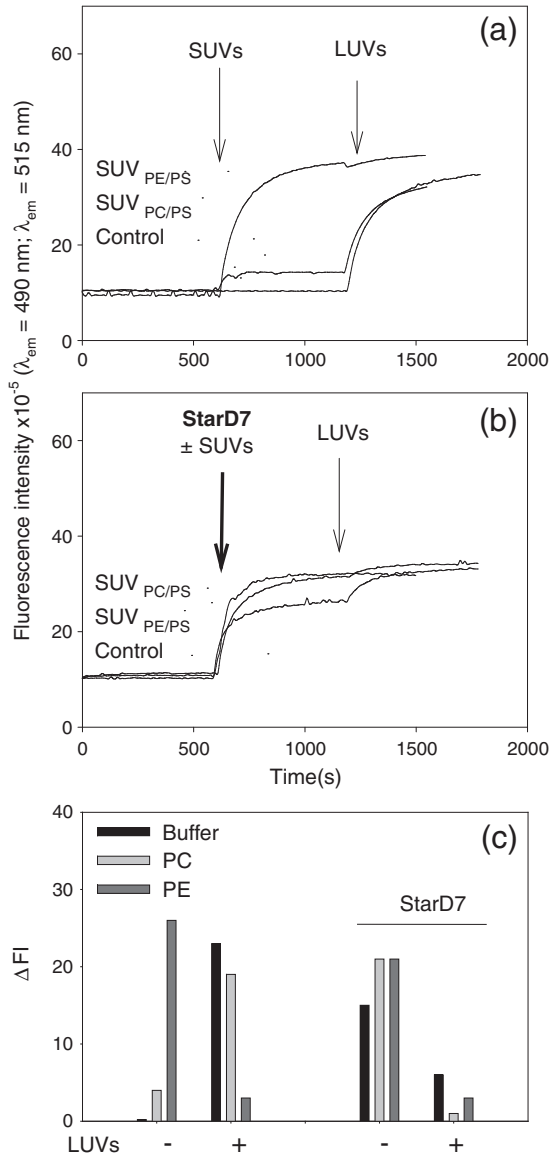

Fig. 7. Effect of the chemical composition of nonlabeled SUVs added on BD-HPC dequenching. At time zero and up to 600 s, samples contained $SUV_{BD\text{-}HPC/PC/PS}$. (a) Addition of nonlabeled $SUV_{PE\text{-}PS}$ or $SUV_{PC\text{-}PS}$ and $LUV_{PS\text{-}PC}$ is indicated by the arrows. (b) Same as in (a) but StarD7 was added alone or simultaneously with nonlabeled SUVs. In the control sample, buffer (a) or StarD7 (b) was added. Fluorescence was recorded at $\lambda_{em} = 515$ nm ($\lambda_{ex} = 490$ nm). (c) $\Delta FI = FI_{t=1000} - FI_{t=0}$ before (−LUVs) or $\Delta FI = FI_{t=1500} - FI_{t=1000}$ or after (+LUVs) the addition of LUVs.

explain the decrease in the fluorescence intensity of BD-HPC as its accessibility to water increases (e.g. at decreasing concentration of dioxane in aqueous solutions such as in Fig. 3).

Taking into account that BD-HPC is an acyl chain-labeled zwitterionic probe, it is expected that in aqueous media, it is either self-assembled or incorporated in a lipid self-assembled structure with the fluorescent moiety embedded within the hydrophobic core of the structure. In addition, the presence of large concentrations of BD-HPC would be expected to impact negatively on its quantum yield through a self-quenching phenomenon [25] which can be relieved upon dilution. Thus, in addition to H-bonding and the stabilization of charge transfer state intermediate, an increased tendency to self-assembling and consequently self-quenching would have contributed to the steeper reduction in the quantum yield as the water content of the solvent increased from 80 to 100% v/v in Fig. 3b.

These results give experimental support to the hypothesis that the increase in BD-HPC fluorescence intensity (FI_{max1} in Fig. 2b) up on the addition of StarD7 to the media containing $SUV_{BD\text{-}HPC/PC/PS}$ can be explained by a binding of BD-HPC either within hydrophobic pockets of StarD7, StarD7 aggregates, or lipid–StarD7 interfaces, which are expected to be dehydrated environments. Thus, through the formation of mixed lipid–protein self-assembled structures, StarD7 would be able to offer a more hydrophobic environment with lower access to water leading to an increase in the quantum yield and at the same time might induce a small dilution-like effect relieving the self-quenching of fluorescence emission. Hence, a monomeric lipid–protein interaction model is not necessary to explain these results.

4.3. Role of electrostatic interactions in the StarD7-induced BD-HPC fluorescence dequenching

Within the bulk pH range assayed the surface charge density of the vesicles used remained negative and constant. Results shown in Fig. 4 (FI_{max1}) suggest that electrostatic interactions seemed not to affect significantly the StarD7–$SUV_{BD\text{-}HPC/PC/PS}$ binding at 1:20 protein/lipid molar ratio. Possibly, at this protein concentration, a high level of protein–lipid binding impaired bilayer fusion revealed by the small changes induced by StarD7 in FI_{max2} values (Fig. 4a). This was partially reversed by a binding partial inhibition induced by phenomena such as buffer change (the osmolarity of Tris–HCl was lower than that of phosphate buffer) or a decrease in protein surface charge at pH 6. However, when surface charges were screened in the presence of high salt concentration (Fig. 4c), only the stages that follow $LUV_{PC\text{-}PS}$ addition, were blocked, and the self-quenching of BD-HPC fluorescence was not released. The participation of StarD7 in this stage depends on electrostatic interactions, as well as on its relative concentration with respect to LUVs (1:600 protein/lipid molar ratio). (Notice that results shown in Fig. 2 correspond to protein/lipid molar ratios that varied from 1:1500 to 1:30,000). From this experiment we conclude that a strong inhibition of StarD7–lipid binding totally abolished the dequenching and possible fusion (Fig. 4c).

4.4. Mechanism of dequenching of BD-HPC fluorescence in the presence of StarD7

An experimental setup similar to that used in the present work has been applied under the assumption that it is the appropriate one to test protein effectiveness as exchangers of lipid molecules in a monomeric form between two membranes [15]. However, membrane fusion may also be a feasible mechanism to explain fluorescence dequenching through lipid dilution (F_{max2} in Fig. 2). To demonstrate that a protein has fusogenic activity, three activities should be demonstrated: a) lipid mixing, b) increase in vesicle size and c) mixing of interior aqueous contents [26,27]. All these conditions were examined to test whether StarD7 had fusogenic potential.

4.4.1. StarD7 induced lipid mixing

Förster energy transfer (FRET) is a probabilistic event based on the radiationless transfer of excitation energy from a donor to an acceptor. FRET depends on the degree of spectral overlap of the donor and acceptor. Moreover, since the interaction between the donor and acceptor is a dipole–dipole interaction, FRET is a distance- and orientation-dependent interaction. The energy transfer occurs typically over a distance of 1–10 nm. Only samples containing StarD7 exhibited the decrease in $FI_{427/515}$ demonstrating that both probes, originally located in different bilayers, approximated within the Förster's distance. This result indicated that in the presence of StarD7 one of the conditions for bilayer membrane fusion, lipid mixing, occurred.

4.4.2. StarD7 promotes an increase in vesicle size

This conclusion is based on the fact that, as reported previously [28], the area of vesicles formed by fusion should be equal to two small vesicles. The resulting radius would be larger than the original

vesicle by a factor of $2^{1/2}$ and the resulting volume would be greater than that of the original vesicle by a factor of $2^{3/2}$ and the sum of the two in $2^{1/2}$. Then, the merging of two equal spherical vesicles would result in an increase of 41% of the volume of two individual vesicles. This rule was followed by the 33 nm SUVs, which after the addition of StarD7 exhibited a mean vesicle size of 47 nm (particle Population I in Table 1). Moreover, another population of 326 nm particles, almost 10 times larger than the original SUVs was observed and these may be explained by the presence of free- or lipid bound-protein aggregates. However, these particles (Population II) represented only a 5.6% of the total particle distribution.

The addition of LUVs to SUVs in the presence of StarD7 produced two populations of vesicles. The more abundant population (87%) with a mean diameter of 48 nm represents fusion between two SUVs (Population I). The second less abundant population (II, 13% abundance) was larger than expected from the fusion of two 107 nm diameter LUVs which would be predicted to have been approximately 150 nm in diameter. The Population II vesicles may represent a complex combination of several particles, including SUVs which are less stable than LUVs.

Compared with SUVs–protein samples, in SUVs–protein–LUVs samples the lipid/protein ratio increased from 286 up to 571 mol/mol. In these experiments, in addition to a smaller (44 nm) and more abundant (93%) population of particles, there was another population of 175 nm diameter. These particles were smaller than those formed in mixtures of SUV–LUV in the absence of StarD7 (202 nm), as well as being smaller than protein aggregates in the absence of lipid (326 nm). This result may be explained by the participation of a higher proportion of SUVs being incorporated into particles in the presence of StarD7 and from the inhibition of protein aggregation due to the higher availability of lipid–water interfaces.

Taken together these results indicate that the SUV–SUV fusion, as well as SUV–LUV fusion can be promoted by both StarD7 and LUVs alone or in combination. The lower particle size of Population II obtained following the addition of StarD7 and LUVs together may indicate the higher proportion of SUVs in the composition of the fused particles, and could explain the more efficient probe dilution (higher fluorescence dequenching) observed in SUVs–protein–LUVs samples compared with SUVs–LUVs (Fig. 2).

4.4.3. StarD7 facilitates mixing of aqueous interior (cell–cell fusion)

To test the third condition to demonstrate that StarD7 is a fusogenic protein, we studied cell–cell fusion by fluorescence microscopy [29]. Since we had determined a partial relocalization of this protein to cytoplasmic membrane during trophoblast differentiation, we selected the human trophoblastic cell line, BeWo, for this assay.

The presence of StarD7 protein induced the formation of multinuclear giant cells (Fig. 6b). This process consists of the fusion of mononuclear undifferentiated cells to form differentiated syncytium-like cells with the loss of intercellular boundaries resulting in the mixing of their cytoplasmic contents at all the StarD7 concentrations tested (Fig. 6c).

Taken together, FRET, DLS and cell–cell interaction experiments allow us to conclude that the dequenching of BD-HPC induced by StarD7 is mediated by a bilayer fusion as all the conditions required to accept a fusogenic effect, i.e. lipid mixing (Fig. 5b), increase in vesicle size (Table 1) and mixing of interior aqueous contents (Fig. 6) have been demonstrated.

4.5. The impact of fusogenic lipids on BD-HPC fluorescence dequenching induced by StarD7

Fusion is a process that involves the participation of intermediate lipid structures (stalk structure) which resemble the well known inverted phases (hexagonal II or cubic phases) [30]. The geometric and thermodynamic conditions required to stabilize such phases can be satisfied by phospholipids having small polar head group area compared with the area occupied by two hydrocarbon chains. Phosphatidylethanolamine joins these properties and when it accompanies other phospholipids in bilayers facilitates their fusion. It is known that aqueous dispersions of unsaturated PE adopt the HII hexagonal structure, while other fusogenic lipids such as unsaturated phosphatidic acid or phosphatidylserine will exist in bilayers unless the headgroup charge is neutralized either by low pH or by the presence of multivalent cations, such as Ca^{2+}. So, PE was chosen for this experiment.

Thus, it is expected that PE containing membranes should be more sensitive to the action of other fusogenic molecules [31]. In the present report SUVs containing PE were used to support fusion as the action mechanism of StarD7 expecting that these membranes would be more prone to follow fusion than $SUV_{PC\text{-}PS}$.

5. Concluding remarks

Curvature stress may be the driving force leading to a reduction in the surface free energy through membrane fusion. This was reflected in our experiments where labeled SUVs were mixed with LUVs at zero StarD7 concentration (Fig. 2). StarD7 may serve to screen electrostatic, steric and hydration forces that create a repulsive barrier between membranes. StarD7 may also facilitate close apposition of membranes and initiate membrane aggregation by lowering the surface charge or the number of water sites thereby diminishing membrane repulsion. The efficiency of lipid dilution depended on StarD7 electrostatic interaction with the lipid–water interface as shown by the pH and salt modulation (Fig. 4). StarD7 binding to PS containing monomolecular layers at the air–water interface had been demonstrated previously [10]. In the present study we showed that, in conditions where electrostatic charges were screened, lipid dilution after LUVs addition was inhibited both in the presence and in the absence of StarD7 (Fig. 4c). In the former case this may reflect the requirement of protein binding as a starting stage of the fusion process, while in the later case a reduction in membrane curvature may stabilize SUVs and may also contribute to the fusion inhibition (see below).

Most membrane fusion in biological systems (e.g. endocytosis, exocytosis, intracellular vesicle trafficking, fertilization, virus entry into the cells, etc.) is induced or mediated by proteins on these membranes, followed by mixing of the membrane lipids. It is assumed that at some point during fusion a pore is formed with proteinaceous or lipidic composition [32]. According to the proteinaceous pore hypothesis, fusion starts with a single proteinaceous channel that later opens into a full fusion pore due to diffusion of the protein components in the lipid bilayer [33]. On the other hand, the lipidic pore hypothesis states that fusion proceeds through a hemifusion event. The latter is a partially fused structure in which lipids mix although aqueous compartments do not and consists of nonlamellar lipid structures such as HII phase. This is the “stalk model”. Siegel proposed a “modified stalk model” in which another type of intermediate structure, the transmembrane contact (TMC), might also be energetically possible [30]. It has been shown that when lipids with positive spontaneous curvature are incorporated into the low radius curvature membrane, it would reduce the surface energy of the positively curved membrane and membrane fusion is suppressed [34–37]. Lipids with positive spontaneous curvature will lower the energy state of membranes of low radius curvature and at the same time will unstabilize or inhibit the HII phase [38] which requires lipids with negative curvature. On the contrary, lipids with negative spontaneous curvature are expected to favor the fusion process. Accordingly, we found that lipid dilution was favored by non-lamellar forming lipids such as PE (Fig. 7) and StarD7 further increased the labeled lipid dilution in the presence of PE containing membranes up to a common maximum. This indicated that StarD7 and PE contributed to lipid dilution through the same mechanism (i.e. membrane fusion). These results in conjunction with the pH and salt sensitivity, as well as the ability of StarD7 to affect the surface pressure and electrostatics in Langmuir films [10] indicated that the protein's surface

activity is the main force driving the whole phenomenon which, through phase changes in bilayers, proceeds toward membrane fusion.

Finally, experiments using vesicles containing PE, as well as FRET, DLS and cell–cell fusion strongly support fusion as the main mechanism leading to fluorescence dequenching through labeled lipid dilution upon StarD7 binding to the lipid–water interface. Present results suggest a possible molecular mechanism and provide experimental support to our proposal that StarD7 may play an important role in the phospholipid-mediated signaling of trophoblastic tumor cellular events, as well as in its effect in promoting membrane fusion in cells.

Acknowledgements

The present work was partially financed by grants from CONICET, SECyT-Universidad Nacional de Córdoba and ANPCyT from Argentina. SA and JMS contributed equally to the present work. SA holds a post-doctoral fellowship from ANPCyT-Argentina. JMS, SG-R and MAP are Career Investigators from CONICET.

References

[1] M. Schramm, M. Korner, G. Neufeld, E. Nedivi, The molecular mechanism of action of the beta-adrenergic receptor, Cold Spring Harb. Symp. Quant. Biol. 48 (1983) 187–191.
[2] H. Caohuy, Membrane Fusion Protein Annexin 7: A Common Site of Action for Calcium, Guanosine Triphosphate, Protein Kinase C and Botulinum Toxin Type C in Regulated Exocytosis in, , 2002.
[3] M. Schramm, Transfer of glucagon receptor from liver membranes to a foreign adenylate cyclase by a membrane fusion procedure, Proc. Natl. Acad. Sci. U. S. A. 76 (1979) 1174–1178.
[4] J.M. White, Membrane fusion: the influenza paradigm, Cold Spring Harb. Symp. Quant. Biol. 60 (1995) 581–588.
[5] A.J. Verkleij, J. Leunissen-Bijvelt, B. de Kruijff, M. Hope, P.R. Cullis, Non-bilayer structures in membrane fusion, CIBA Found. Symp. 103 (1984) 45–59.
[6] S.L. Roderick, W.W. Chan, D.S. Agate, L.R. Olsen, M.W. Vetting, K.R. Rajashankar, D.E. Cohen, Structure of human phosphatidylcholine transfer protein in complex with its ligand, Nat. Struct. Mol. Biol. 9 (2002) 507–511.
[7] J.C. Holthuis, T.P. Levine, Lipid traffic: floppy drives and a superhighway, Nat. Rev. Mol. Cell Biol. 6 (2005) 209–220.
[8] M.J. Romanowski, R.E. Soccio, J.L. Breslow, S.K. Burley, Crystal structure of the *Mus musculus* cholesterol-regulated START protein 4 (StarD4) containing a StAR-related lipid transfer domain, Proc. Natl. Acad. Sci. 99 (2002) 6949–6954.
[9] Y. Tsujishita, J.H. Hurley, Structure and lipid transport mechanism of a StAR-related domain, Nat. Struct. Biol. 7 (2000) 408–414.
[10] S. Angeletti, B. Maggio, S. Genti-Raimondi, Surface activity and interaction of StarD7 with phospholipid monolayers, Biochem. Biophys. Res. Commun. 314 (2004) 181–185.
[11] Y. Horibata, H. Sugimoto, StarD7 mediates the intracellular trafficking of phosphatidylcholine to mitochondria, J. Biol. Chem., 285 7358–7365
[12] S. Angeletti, V. Rena, R. Nores, R. Fretes, G.M. Panzetta-Dutari, S. Genti-Raimondi, Expression and localization of StarD7 in trophoblast cells, Placenta 29 (2008) 396–404.
[13] R.R. Adler, A.K. Ng, N.S. Rote, Monoclonal antiphosphatidylserine antibody inhibits intercellular fusion of the choriocarcinoma line, JAR, Biol. Reprod. 53 (1995) 905–910.
[14] L. Feng, W.W. Chan, S.L. Roderick, D.E. Cohen, High-level expression and mutagenesis of recombinant human phosphatidylcholine transfer protein using a synthetic gene: evidence for a C-terminal membrane binding domain†, Biochemistry 39 (2000) 15399–15409.
[15] M.D. Esposti, J.T. Erler, J.A. Hickman, C. Dive, Bid, a widely expressed proapoptotic protein of the Bcl-2 family, displays lipid transfer activity, Mol. Cell. Biol. 21 (2001) 7268–7276.
[16] J. Pereira-Lachataignerais, R. Pons, P. Panizza, L. Courbin, J. Rouch, O. López, Study and formation of vesicle systems with low polydispersity index by ultrasound method, Chem. Phys. Lipids 140 (2006) 88–97.
[17] R.C. MacDonald, R.I. MacDonald, B.P.M. Menco, K. Takeshita, N.K. Subbarao, L.-r. Hu, Small-volume extrusion apparatus for preparation of large, unilamellar vesicles, Biochim. Biophys. Acta (BBA) — Biomembranes 1061 (1991) 297–303.
[18] D.A. Garcia, M.A. Perillo, Benzodiazepine localisation at the lipid–water interface: effect of membrane composition and drug chemical structure, Biochim. Biophys. Acta (BBA) — Biomembranes 1418 (1999) 221–231.
[19] I.D. Johnson, H.C. Kang, R.P. Haugland, Fluorescent membrane probes incorporating dipyrrometheneboron difluoride fluorophores, Anal. Biochem. 198 (1991) 228–237.
[20] J. Karolin, L.B. Johansson, L. Strandberg, T. Ny, Fluorescence and absorption spectroscopic properties of dipyrrometheneboron difluoride (Bodipy) derivatives in liquids, lipid–membranes, and proteins, J. Am. Chem. Soc. 116 (1994) 7801–7806.
[21] R. Bauer, M. Hansen, S. Hansen, L. Ogendal, S. Lomholt, K. Qvist, D. Horne, The structure of casein aggregates during renneting studied by indirect Fourier transformation and inverse Laplace transformation of static and dynamic light scattering data, respectively, J. Chem. Phys. 103 (1995) 2725–2737.
[22] A. Vargas, J. Moreau, S.b. Landry, F.d.r. LeBellego, C. Toufaily, Ã.r. Rassart, J. Lafond, B. Barbeau, Syncytin-2 plays an important role in the fusion of human trophoblast cells, J. Mol. Biol. 392 (2009) 301–318.
[23] V.N. Uversky, Use of fast protein size-exclusion liquid chromatography to study the unfolding of proteins which denature through the molten globule, Biochemistry 32 (1993) 13288–13298.
[24] P.L. Muino, P.R. Callis, Solvent effects on the fluorescence quenching of tryptophan by amides via electron transfer. Experimental and computational studies, J. Phys. Chem. B 113 (2009) 2572–2577.
[25] M. Dahim, N.K. Mizuno, X.-M. Li, W.E. Momsen, M.M. Momsen, H.L. Brockman, Physical and photophysical characterization of a BODIPY phosphatidylcholine as a membrane probe, Biophys. J. 83 (2002) 1511–1524.
[26] S. Massari, R. Colonna, Membrane fusion: studies with model systems, Ann. Ist. Super. Sanita 24 (1988) 59–69.
[27] R.F. Epand, U. Schlattner, T. Wallimann, M.-L. Lacombe, R.M. Epand, Novel lipid transfer property of two mitochondrial proteins that bridge the inner and outer membranes, Biophys. J. 92 (2007) 126–137.
[28] J. Wilschut, D. Hoekstra, Membrane fusion: lipid vesicles as a model system, Chem. Phys. Lipids 40 (1986) 145–166.
[29] F.S. Cohen, G.B. Melikyan, Methodologies in the study of cell–cell fusion, Methods 16 (1998) 215–226.
[30] D.P. Siegel, The modified stalk mechanism of lamellar/inverted phase transitions and its implications for membrane fusion, Biophys. J. 76 (1999) 291–313.
[31] L.V. Chernomordik, M.M. Kozlov, Protein–lipid interplay in fusion and fission of biological membranes, Annu. Rev. Biochem. 72 (2003) 175–207.
[32] B.R. Lentz, Seeing is believing: the stalk intermediate, Biophys. J. 91 (2006) 2747–2748.
[33] M. Lindau, W. Almers, Structure and function of fusion pores in exocytosis and ectoplasmic membrane fusion, Curr. Opin. Cell Biol. 7 (1995) 509–517.
[34] L.V. Chernomordik, S.S. Vogel, A. Sokoloff, H.O. Onaran, E.A. Leikina, J. Zimmerberg, Lysolipids reversibly inhibit Ca2+-, GTP- and pH-dependent fusion of biological membranes, FEBS Lett. 318 (1993) 71–76.
[35] L. Chernomordik, M. Kozlov, J. Zimmerberg, Lipids in biological membrane fusion, J. Membr. Biol. 146 (1995) 1–14.
[36] I. Martin, J.M. Ruysschaert, Lysophosphatidylcholine inhibits vesicles fusion induced by the NH2-terminal extremity of SIV/HIV fusogenic proteins, Biochim. Biophys. Acta (BBA) — Biomembranes 1240 (1995) 95–100.
[37] S. Ohki, G.A. Baker, P.M. Page, T.A. McCarty, R.M. Epand, F.V. Bright, Interaction of influenza virus fusion peptide with lipid membranes: effect of lysolipid, J. Membr. Biol. 211 (2006) 191–200.
[38] M.A. Perillo, N.J. Scarsdale, R.K. Yu, B. Maggio, Modulation by gangliosides of the lamellar-inverted micelle (hexagonal II) phase transition in mixtures containing phosphatidylethanolamine and dioleoylglycerol, Proc. Natl. Acad. Sci. 91 (1994) 10019–10023.